PCCP

Physical Chemistry Chemical Physics

This paper is published as part of a PCCP Themed Issue on:

Nanophotonics: Plasmonics and Metal Nanoparticles

Guest Editors: Greg V. Hartland (University of Notre Dame) and Paul Mulvaney (University of Melbourne)

Editorial

Communication

Papers

The effect of surface roughness on the plasmonic response of individual sub-micron gold spheres†

Jessica Rodríguez-Fernández,*[ab] Alison M. Funston,*[b] Jorge Pérez-Juste,[a] Ramón A. Álvarez-Puebla,[a] Luis M. Liz-Marzán[a] and Paul Mulvaney[b]

Received 13th March 2009, Accepted 8th April 2009
First published as an Advance Article on the web 15th May 2009
DOI: 10.1039/b905200n

Nanoscale surface corrugation strongly determines the plasmonic response of gold nanoparticles with dimensions of several tens of nanometres. Scattering spectra of individual spheres with a rough surface were found to red-shift and broaden. The plasmon modes exhibited quadrupole damping, in contrast to particles with smooth surfaces. Additionally, rougher spheres display a higher SERS activity, which demonstrates the crucial role of nanoscale surface texturing on the plasmonic response of gold particles.

Introduction

The excitation of localized surface plasmon resonances in nanometre-sized metallic particles is appealing for a variety of applications since they possess unique, highly tunable, optical properties in the visible and near infrared (NIR) regions of the spectrum. The synthesis of nanocrystals with tailored plasmon energies not only demands the fine-tuning of particle size and morphology, but also the identification and quantification of the intrinsic factors governing plasmon excitation: specifically the particle size, shape and composition.[1–3] Additionally, as observed with macroscopic metallic surfaces,[4] the extent of surface plasmon excitation in subwavelength metal nanoparticles is strongly influenced by the surface topography. So far, only a few recent studies have explored the relationship between surface roughness (or porosity) and optical response. For instance, Halas and co-workers investigated the effect of surface texturing on the optical properties of submicrometre gold nanoshells,[5,6] as well as on Au "meatball-like" spheres.[7] For both types of mesoscopic corrugated particles, damping of the higher-order plasmon modes and spectral shifts were claimed to occur. In a latter theoretical work, Pecharromán *et al.* postulated that even atomic scale surface roughness could induce significant red shifts in the longitudinal plasmon band of small Au nanorods.[8] Recently, this behaviour has been observed in highly corrugated[9] (micron) and highly porous[10] (submicron) Au rods. However, in all these works, the optical effects resulting from surface roughness are obtained as an average over all the particles in the colloidal solution. Since surface corrugation varies from particle-to-particle, a combined morphological and optical investigation at the single particle level would be highly desirable. Dark-field microspectroscopy (DFM) has become one of the most widely used techniques for single particle spectroscopy investigations in Au,[11,12] Ag[13,14] and even Ni colloids.[15] In combination with electron microscopy imaging, it has allowed the elucidation of the size and shape-dependent scattering response of several types of individual nanocrystals.[16–21]

Nanoscale surface texturing in metal nanoparticles can lead to significantly higher local field enhancement factors compared to those obtained with smooth particles.[5,22] The electromagnetic enhancement is one of the principal mechanisms contributing to surface enhanced Raman scattering (SERS).[23,24] Thus, the optical enhancement exhibited by these corrugated nanostructures makes them promising candidates for applications such as SERS detection.[7,25]

In this paper we investigate (qualitatively) the effect of nanoscale surface corrugation on the optical far-field and near-field performance of spherical Au colloids of various sizes, between 100 and 200 nm. The far-field (Rayleigh) scattering of corrugated/uncorrugated Au spheres of various sizes was tracked at the single nanocrystal level by means of DFM/SEM on each particle,[17] whereas the optical amplification was probed through ensemble SERS, *i.e.* SERS from an ensemble of colloidal particles characterized by a stable average spectrum with well defined frequency and bandwidth.[26] Our results clearly demonstrate that surface corrugation plays a major role in their plasmonic response.

Experimental

Chemicals

Tetrachloroauric acid $HAuCl_4{\cdot}3H_2O$, trisodium citrate dihydrate, cetyltrimethylammonium bromide (CTAB), L-ascorbic acid, poly(methyl methacrylate) (PMMA, M_w 120 000 g mol^{-1}) and polyvinylpyrrolidone (PVP, M_w 40 000 g mol^{-1}) were purchased from Aldrich. Mercaptopolyethyleneglycol (PEG-SH, M_w 5000 g mol^{-1}) was procured from Fluka. All reactants were used without further purification. Milli-Q grade water was used in all the preparations.

[a] *Departamento de Química Física and Unidad Asociada CSIC-Universidade de Vigo, 36310 Vigo, Spain. E-mail: jesica@uvigo.es; Fax: +34 9 8681 2556*
[b] *School of Chemistry & Bio21 Institute, University of Melbourne, Parkville, VIC, 3010, Australia. E-mail: afunston@unimelb.edu.au; Fax: +61 3 9348 1595*

† Electronic supplementary information (ESI) available: Representative TEM micrographs and size distributions of the spherical Au colloids studied by DFM/SEM. See DOI: 10.1039/b905200n

Synthesis of Au spheres

Three colloid samples containing gold spheres in CTAB solution (average diameters: 120, 150 and 197 nm from TEM measurements) were prepared according to the seeded-growth method described by Rodríguez-Fernández *et al.*[27] Additional aqueous dispersions of commercial gold spheres (111, 159 and 198 nm size from TEM measurements) were procured from BB International. The particles synthesised in-house showed corrugated surfaces and accordingly they will be referred to as ''rough'' hereafter; whereas the commercial ones, with smoother surfaces, will be termed ''smooth''.

Sample preparation for single particle spectroscopy

ITO (indium tin oxide) coated glass substrates (Delta Technologies, Ltd.) were cleaned (30 min sonication in 2-propanol), dried with an air stream and spin-coated (3 s, 5000 rpm) with 30 μL of a PMMA solution (1%, in chloroform). The polymer was allowed to dry for at least 2 h at room temperature. In order to reduce the scattering contribution from the surfactant (CTAB), each gold colloid was centrifuged and redispersed in water. For the commercial samples, the 111 nm colloids were used as received, whilst the ligands of the larger 159 nm and 198 nm samples were exchanged with polyvinylpyrrolidone (PVP) or mercaptopolyethyleneglycol (PEG-SH), respectively, to improve particle dispersion in the films. Subsequently, 30–200 μL of the clean dispersions were spin-coated (5 s, 3000 rpm) on the PMMA-modified ITO substrates.

Substrate marking

The as-prepared substrates containing deposited gold nanoparticles were etched using the focused ion beam (FIB) registration method reported by Novo *et al.*,[17] which facilitates the identification and localisation of the gold nanoparticles within a specific area, both under dark-field illumination and scanning electron microscopy (SEM). Box-like patterns (50 μm × 50 μm in size, 1 μm in depth) were milled using the FIB functionality of an xT Nova NanoLab SEM. For each box the corner etchings were unique to allow unequivocal identification.

Single particle spectroscopy and imaging

Gold nanoparticles located inside and around the box area were imaged and their scattering spectra acquired using a 100 W halogen lamp illumination source on a Nikon Eclipse TE-2000 inverted optical microscope coupled to a Nikon Dark-field Condenser (Dry, 0.95–0.80 NA). The scattered light from each nanocrystal was collected with a Nikon Plan Fluor ELWD 40×/0.60 NA objective and focused onto the entrance slit of a MicroSpec 2150i imaging spectrometer coupled with a TE-cooled CCD camera (PIXIS 1024B ACTON Princeton Instruments). The acquisition time was 6–60 s depending upon the sample, the larger spheres required a shorter collection time. To allow a direct correlation between particle position on the substrate and the corresponding spectrum, the box and adjacent areas were imaged and mapped in the DFM. Subsequently, the same particles were identified and imaged using an SEM xT Nova NanoLab. All the scattering spectra were corrected dividing by the background collected from an adjacent region without particles. Particles with ellipticity >1.1 were discarded during post-processing of the data.

Optical modelling

Scattering spectra of spherical Au particles of various sizes were calculated according to generalized Mie theory based on multiple elastic scattering of multipole expansions (MESME).[28,29] The gold dielectric data were taken from Johnson and Christy.[30] The surrounding medium was accounted for by considering the particles to be embedded in a homogeneous medium with an effective refractive index, $n_{\mathrm{eff}} = 1.25$, equal to the mean of air ($n = 1$) and the substrate/PMMA layer ($n = 1.5$). In order to evaluate the effect of the substrate on the calculated optical properties of the gold nanoparticles, additional simulations[2] (not shown) were performed on gold spheres of various sizes supported on silica substrates. The influence of illumination under dark-field conditions was also evaluated. This involved calculation of the integrated scattering spectra over the range of angles of incidence produced by the dark field condenser, from $\theta = 53^\circ$ to $\theta = 72^\circ$, and over all the azimuthal angles ($\phi = [0–360^\circ]$). The light was assumed to be collected along the sample normal in all cases.

SERS measurements

SERS spectra were recorded with a LabRam HR (Horiba-Jobin Yvon) Raman instrument. Prior to the SERS experiments the Au and CTAB concentrations in all the colloidal dispersions (rough and smooth) were adjusted to 0.25 mM and 1 mM, respectively. 1-Naphthalenethiol (1-NAT, Acros Organics) was used as a Raman probe. Typically, 1-NAT (at a final concentration of 10^{-5} M) was added to each gold colloid solution and allowed to chemisorb overnight. Average SERS spectra of the colloidal suspensions were collected with excitation at either 633 nm (He–Ne) or 785 nm (diode) in backscattering geometry using a macro-sampling 90° objective adaptor. Spectra were collected with accumulation times of 10 s.

Results and discussion

Spherical gold colloids were synthesized through seed-mediated growth of smaller nuclei in an aqueous CTAB solution.[27] Representative TEM micrographs and size distributions are provided in the ESI (Fig. S1).† This protocol yields spherical nanoparticles of pre-determined size, with low ellipticity, narrow size distribution and well-defined optical response. In particular, three samples with 120, 150 and 197 nm average (TEM) diameter were investigated. The optical (scattering) and morphological properties of individual Au spheres from the three batches were investigated by DFM and SEM on each nanoparticle. This protocol permits a direct evaluation of the single particle optical response and correlation with the particle's morphological features. Representative scattering spectra and correlated high-resolution SEM images on the same Au nanosphere are shown in Fig. 1(A–C). These micrographs show considerable inhomogeneities (nanoscale corrugation) on the surfaces of the nanocrystals, in clear

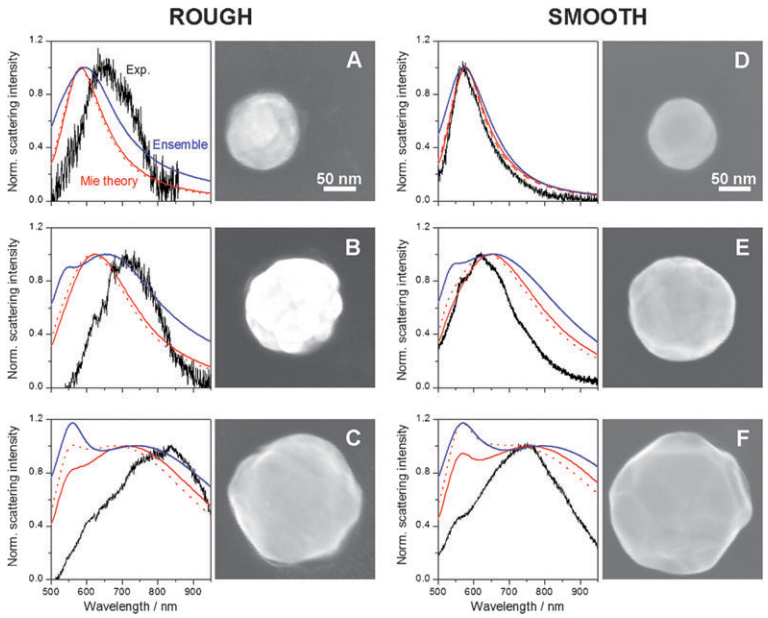

Fig. 1 Representative scattering spectra/SEM micrographs of single Au spheres with either corrugated (A–C) or smooth (D–F) surfaces. The particle diameters as well as the dipole and quadrupole resonance wavelengths are summarized in Table 1. The light (red in the electronic version) curves show the scattering cross section of each particle, as calculated from Mie theory with (dashed) and without (solid) consideration of the illuminating cone directions, for light collection along the sample normal. The corresponding ensemble spectra (in water) are superimposed as a darker (blue in the electronic version) solid line. All the spectra were normalized at the dipole maximum wavelength to facilitate comparison.

contrast to the apparent surface smoothness previously reported after low-resolution SEM characterization.[27] In all cases, the scattering spectra exhibit a well-defined and broad dipolar plasmon resonance band that red-shifts as the particle size is increased. In the spectrum of the largest imaged sphere ($<\phi>$ = 199 nm, Fig. 1C), a shoulder at lower wavelengths (ascribed to a quadrupolar mode[27]) is also apparent.

However, the scattering response from these particles deviates notably from the spectra calculated using Mie theory (spectra superimposed in the same plots). The experimental spectra are considerably red-shifted, and exhibit broadening in some cases, of the dipolar (or quadrupolar) mode. In addition, the plasmon energies of the individual particles systematically lie below the ensemble peak wavelength (in water, n = 1.33). This occurs even though the average refractive index around the single particles (supported on PMMA-modified ITO substrates) is lower (*ca.* n = 1.25). Such anomalous behaviour could be readily ascribed to the observed texturing of the nanocrystal surface. However, additional factors, such as the conditions of the dark-field illumination (hollow cone of light impinging on the sample) or the supporting substrate could also contribute.

The influence of both factors was evaluated theoretically. First, it was confirmed that the annular dark-field illumination (between 53–72° from the normal to the substrate, see the Experimental section for details) in the calculated spectra has almost no effect on the response of the smaller particles (120 and 150 nm, Fig. 1A and B, respectively). For the larger sphere (199 nm, Fig. 1C), just a slight blue-shift of the dipole and an increase in the quadrupole intensity are predicted theoretically. The substrate only induces a slight red shift in the simulations, compared to unsupported particles in air[2] (simulations not shown). We can therefore conclude that neither the specific dark-field illumination conditions, nor the effect of the substrate can explain the strongly red-shifted experimental spectra. As a consequence, the surface texturing (evident in the SEM images) is concluded to be the main contributing factor to the experimentally observed deviations from the calculated spectra.

To further explore the role of surface roughness on the optical properties of individual Au spheres we also investigated three additional samples (111, 159 and 198 nm average TEM diameter) of gold spheres with smooth surfaces using DFM/SEM. Representative results are given in Fig. 1(D–F) and further summarized in Table 1. Indeed, all the particles show well-defined and narrower plasmon resonances with energies in good agreement with Mie theory, in contrast to the corrugated particles. Obviously, nanoscale surface texturing leads to considerable peak-broadening and red-shifting of the single particle plasmon resonances. However, the fact that the rough spheres show red-shifted spectra at the single particle level is not evident from the ensemble spectrum, which actually agrees well with the calculated extinction in water (not shown).[27] Moreover, no significant differences are observed in the ensemble absorption spectra of corrugated/smooth Au spheres of the same average size. Both observations indicate that surface roughness does not change the extinction properties of the ensemble significantly (at least for the degree of surface texturing observed in our experiments) as also reported by Halas and co-workers for Au nanoshells.[6] The red shift in the spectra of individual rough particles (in air, *ca.* n = 1.25) *vs.* the ensemble (in water, n = 1.33) could be explained on the basis of "hot spots" (local surface sites where the electric-field is highly localized and enhanced) created on the textured sphere upon light excitation, an effect also reported for gold nanoshells.[5] The "hot spots" touching or

Table 1 Diameter, dipole and quadrupole resonance wavelengths of the corrugated/smooth Au spheres shown in Fig. 1

ROUGH				SMOOTH			
Image	Diameter/nm	$\lambda_{max,dipole}$/nm	$\lambda_{max,quadrupole}$/nm	Image	Diameter/nm	$\lambda_{max,dipole}$/nm	$\lambda_{max,quadrupole}$/nm
A	120	650	—	**D**	114	569	—
B	150	714	—	**E**	165	618	567
C	199	836	598	**F**	214	746	557

in close proximity to the substrate may interact very efficiently with it, resulting in a dramatic red shift of the dipolar mode,[31] which does not occur in the averaged ensemble situation, where the particles are embedded in a truly homogeneous medium.

The effect of nanoscale surface roughness is further illustrated in Fig. 2, where the Rayleigh scattering spectra of two gold spheres (rough and smooth) of the same size are compared. It is clear that the spectrum of the rough sphere is red-shifted and broadened (due to roughness-induced plasmon damping) as discussed above. The size-dependent effect of surface corrugation on the dipole and quadrupole plasmon wavelengths, as measured in single particles, is depicted in Fig. 3. Comparison with the results from Mie theory reveals the anomalous behaviour of the rough spheres, whereas the spectra of smooth particles agree well with the theoretical predictions. In all cases, regardless of surface structure, the dipole mode of the Au spheres undergoes a red shift with increasing particle diameter. The same holds for the quadrupolar mode, which is less sensitive and therefore shows smaller shifts.[32] Interestingly, the quadrupole is observed on very few corrugated spheres (just a few points in Fig. 3), appearing as a weak shoulder in most cases (see *e.g.* Fig. 1C). This differs from the smooth particles, which in most cases show well-defined quadrupolar bands (see *e.g.* Fig. 1E). This observation is also in agreement with the angle-dependent light scattering investigations and FDTD calculations on gold nanoshells[5,6] and Au "meatballs",[7] where damping of the higher-order plasmonic modes due to nanoscale surface roughness is reported by the authors. In addition, the random nature of surface roughness might justify the large spread of dipole wavelengths for Au spheres of similar size. In fact, in our experiments, the 150 nm sample (*e.g.* Fig. 1B), which exhibits particularly high surface corrugation, is the sample which displays the widest spread of dipole mode energies.

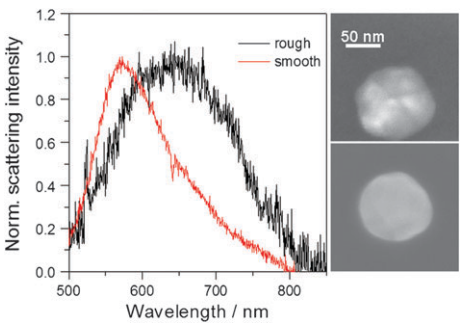

Fig. 2 Normalized scattering spectra of two gold spheres of the same size (⟨diameter⟩ = 111 nm) and ellipticity (*ca.* 1.05), but different surface roughness, as observed in the SEM images: rough (upper panel) and smooth (lower panel). The bands are centred at 642 and 572 nm, respectively.

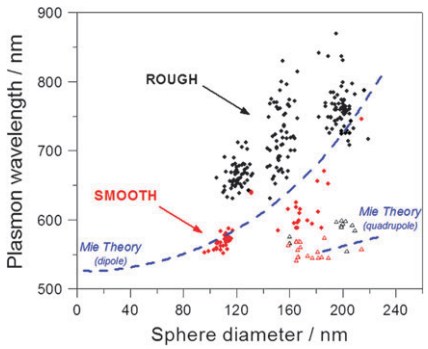

Fig. 3 Size-dependence of the dipole (circles) and quadrupole (triangles) plasmon resonance wavelengths in rough (dark/black) and smooth (light/red in the electronic version) Au spheres, as characterized by correlated DFM/SEM. The theoretical data calculated from Mie theory (with no consideration of the experimental dark-field illumination conditions) are also shown.

So far we have demonstrated the strong influence of nanoscale surface corrugation on the single particle response of spherical gold nanoparticles. However, the presence of such nanoscale protuberances on the particle surfaces is expected to modify not only their far-field response, but also to promote local near-field enhancements[5] that might increase their SERS efficiency. Therefore, we investigated the SERS performance of corrugated and smooth colloids, using 1-naphthalenethiol (1-NAT) as a model analyte[33] that covalently binds to the Au surface atoms through the thiol group. We evaluated the average SERS activity in solution of three corrugated (113, 158 and 190 nm) and three smooth (102, 159 and 198 nm average TEM diameter) samples, displaying the characteristic single particle response described previously. The electrostatic stabilizer of the commercial (smooth) samples was exchanged with CTAB (with no change in the colloid stability) to ensure that the chemical nature of the stabilizer in rough *vs.* smooth samples did not play a role.

Representative SERS spectra of 1-NAT after excitation with both 633 and 785 nm laser lines are displayed in Fig. 4A. The spectra are dominated by the ring stretching (1553, 1503 and 1368 cm^{-1}), CH bending (1197 cm^{-1}), ring breathing (968 and 822 cm^{-1}), ring deformation (792, 664, 539 and 517 cm^{-1}) and CS stretching (389 cm^{-1}) modes.[33] The SERS activity of the different samples was compared by monitoring the intensity of the ring stretching band at 1368 cm^{-1}. SERS amplification per particle (Fig. 4B and C) was obtained by normalizing the intensity of the ring stretching mode to the number of gold particles in each sample. For both samples, smooth and corrugated, the SERS intensity recorded upon excitation with both laser lines increases with particle size, in full agreement with the recent literature.[34,35] However, it is clear that regardless

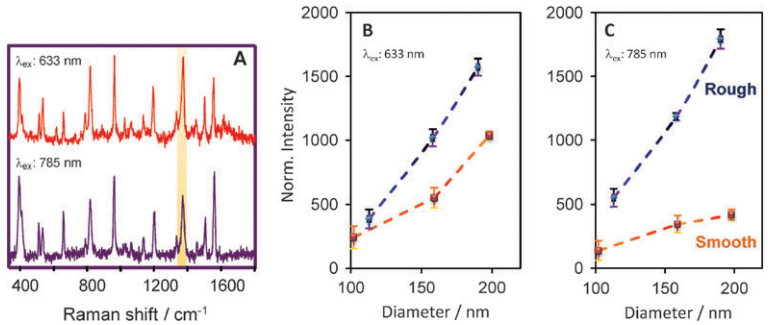

Fig. 4 (A) SERS spectrum of 1-naphthalenethiol (λ_{ex} = 633, 785 nm) chemisorbed on spherical Au colloids. Size dependence of the intensity (normalized to the number of scattering centers) of the 1368 cm^{-1} ring stretching band of 1-NAT, highlighted in (A), when chemisorbed on either a smooth or corrugated gold sphere: excitation with the 633 nm (B) and 785 nm (C) laser lines.

of the excitation wavelength, a higher SERS amplification was consistently obtained from the more corrugated particles. This results in an increase from 2 up to 5 fold in SERS intensity, depending on particle size and laser wavelength. The higher performance of the rough particles is likely to stem from the following factors: (a) the increase of the surface area due to corrugation; (b) the better plasmon-laser line coupling;[36] and, (c) focussing of the electromagnetic fields at the apices of the small tips formed due to the corrugation.[37] SEM images (*cf*. Fig. 1A–C) clearly reveal that the increase in surface area of the rough colloids is insufficient to explain the differences in SERS signal amplification shown in Fig. 4B and C. Moreover, single particle localized surface plasmon spectra (Fig. 1) show that excitation with the 633 nm laser line better overlaps the plasmon as the particle size increases in the smooth spheres and therefore SERS intensity increases. However, in the case of corrugated colloids, 633 nm irradiation only weakly excites the surface plasmon mode of the smaller colloid, while in the other samples it lies on the blue side of the plasmon bands. Unexpectedly, the SERS intensity still increases, showing that amplification in this case may be due to electromagnetic focussing at the apex of the generated tips. This is further confirmed upon excitation with the NIR line (785 nm). The smooth spheres show an increase in SERS intensity as a consequence of the better plasmon-laser coupling as described previously.[38] However, rough colloids show a much stronger increase, due to both plasmon-laser line overlap and plasmon focussing at the tips. Thus, focussing of the electromagnetic field due to the textured surface topography seems to have a significant influence on the SERS amplification by corrugated colloids.

Conclusions

We have demonstrated that nanoscale surface corrugation plays a major role on the localized surface plasmon response of spherical gold colloids. We have shown that the far-field (scattering) spectra of individual Au particles are extremely sensitive to the particle surface topography. Corrugation (even if small) induces a very significant red shift and broadening of the localized surface plasmon resonance, along with damping of the quadrupolar mode. Surface texturing also modifies the near-field enhancing properties of the particles. The rough particles show higher SERS performance, compared to the smooth ones, and their activity is size dependent (with the SERS enhancement increasing with particle size).

Acknowledgements

The authors thank Sergey Rubanov for assistance with SEM/FIB measurements. The Spanish MiCInn is acknowledged for funding an F.P.U. scholarship (J.R.-F.) and Grants PCI2005-A7-0075 and MAT2007-62696 (L.M.L.-M.) and MAT2008-05755 (R.A.A.-P.). P.M. acknowledges support through ARC Fellowship FF0561486 and DEST Grant CG110036.

References

1 K. L. Kelly, E. Coronado, L. L. Zhao and G. C. Schatz, *J. Phys. Chem. B*, 2003, **107**, 668–677.
2 V. Myroshnychenko, J. Rodríguez-Fernández, I. Pastoriza-Santos, A. M. Funston, C. Novo, P. Mulvaney, L. M. Liz-Marzán and F. J. García de Abajo, *Chem. Soc. Rev.*, 2008, **37**, 1792–1805.
3 L. M. Liz-Marzán, *Langmuir*, 2006, **22**, 32–41.
4 H. Raether, *Surface Plasmons on Smooth and Rough Surfaces and on Gratings*, Springer, Berlin, 1988.
5 H. Wang, G. P. Goodrich, F. Tam, C. Oubre, P. Nordlander and N. J. Halas, *J. Phys. Chem. B*, 2005, **109**, 11083–11087.
6 H. Wang, K. Fu, R. A. Drezek and N. J. Halas, *Appl. Phys. B*, 2006, **84**, 191–195.
7 H. Wang and N. J. Halas, *Adv. Mater.*, 2008, **20**, 820–825.
8 C. Pecharromán, J. Pérez-Juste, G. Mata-Osoro, L. M. Liz-Marzán and P. Mulvaney, *Phys. Rev. B*, 2008, **77**, 035418–035417.
9 M. J. Banholzer, S. Li, J. B. Ketter, D. I. Rozkiewicz, G. C. Schatz and C. A. Mirkin, *J. Phys. Chem. C*, 2008, **112**, 15729–15734.
10 H.-M. Bok, K. L. Shuford, S. Kim, S. K. Kim and S. Park, *Nano Lett.*, 2008, **8**, 2265–2270.
11 C. Sönnichsen, T. Franzl, T. Wilk, G. von Plessen and J. Feldmann, *New J. Phys.*, 2002, **4**, 93.
12 C. Novo, D. Gómez, J. Pérez-Juste, Z. Zhang, H. Petrova, M. Reismann, P. Mulvaney and G. V. Hartland, *Phys. Chem. Chem. Phys.*, 2006, **8**, 3540–3546.
13 L. J. Sherry, S. H. Chang, G. C. Schatz, R. P. Van Duyne, B. J. Wiley and Y. Xia, *Nano Lett.*, 2005, **5**, 2034–2038.
14 L. J. Sherry, R. Jin, C. A. Mirkin, G. C. Schatz and R. P. VanDuyne, *Nano Lett.*, 2006, **6**, 2060–2065.
15 J. J. Mock, S. J. Oldenburg, D. R. Smith, D. A. Schultz and S. Schultz, *Nano Lett.*, 2002, **2**, 465–469.
16 J. J. Mock, M. Barbic, D. R. Smith, D. A. Schultz and S. Schultz, *J. Chem. Phys.*, 2002, **116**, 6755–6759.
17 C. Novo, A. M. Funston, I. Pastoriza-Santos, L. M. Liz-Marzán and P. Mulvaney, *Angew. Chem., Int. Ed.*, 2007, **46**, 3517–3520.
18 K. Munechika, J. M. Smith, Y. Chen and D. S. Ginger, *J. Phys. Chem. C*, 2007, **111**, 18906–18911.

19 C. L. Nehl, N. K. Grady, G. P. Goodrich, F. Tam, N. J. Halas and J. H. Hafner, *Nano Lett*., 2004, **4**, 2355–2359.
20 C. L. Nehl, H. Liao and J. H. Hafner, *Nano Lett*., 2006, **6**, 683–688.
21 L. Yang, B. Yan and B. M. Reinhard, *J. Phys. Chem. C*, 2008, **112**, 15989–15996.
22 C. Oubre and P. Nordlander, *J. Phys. Chem. B*, 2004, **108**, 17740–17747.
23 S. J. Lee, Z. Guan, H. Xu and M. Moskovits, *J. Phys. Chem. C*, 2007, **111**, 17985–17988.
24 G. C. Schatz, M. A. Young and R. P. Van Duyne, *Electromagnetic Mechanism of SERS, in Surface-Enhanced Raman Scattering: Physics and Applications*, Berlin, 2006.
25 J. Xie, Q. Zhang, J. Y. Lee and D. I. C. Wang, *ACS Nano*, 2008, **2**, 2473–2480.
26 R. F. Aroca, R. A. Álvarez-Puebla, N. Pieczonka, S. Sánchez-Cortez and J. V. García-Ramos, *Adv. Colloid Interface Sci*., 2005, **116**, 45–61.
27 J. Rodríguez-Fernández, J. Pérez-Juste, F. J. García de Abajo and L. M. Liz-Marzán, *Langmuir*, 2006, **22**, 7007–7010.
28 F. J. García de Abajo, *Phys. Rev. Lett*., 1999, **82**, 2776–2779.
29 F. J. García de Abajo, *Phys. Rev. B*, 1999, **60**, 6086.
30 P. B. Johnson and R. W. Christy, *Phys. Rev. B*, 1972, **6**, 4370–4379.
31 B. Khlebtsov, A. Melnikov, V. Zharov and N. Khlebtsov, *Nanotechnology*, 2006, **17**, 1437–1445.
32 J. Rodríguez-Fernández, I. Pastoriza-Santos, J. Pérez-Juste, F. J. García de Abajo and L. M. Liz-Marzán, *J. Phys. Chem. C*, 2007, **111**, 13361–13366.
33 R. A. Álvarez-Puebla, D. S. Dos Santos and R. F. Aroca, *Analyst*, 2004, **129**, 1251–1256.
34 P. N. Njoki, I. I. S. Lim, D. Mott, H.-Y. Park, B. Khan, S. Mishra, R. Sujakumar, J. Luo and C.-J. Zhong, *J. Phys. Chem. C*, 2007, **111**, 14664–14669.
35 R. A. Álvarez-Puebla, R. Contreras-Cáceres, I. Pastoriza-Santos, J. Pérez-Juste and L. M. Liz-Marzán, *Angew. Chem., Int. Ed*., 2009, **48**, 138–143.
36 A. D. McFarland, M. A. Young, J. A. Dieringer and R. P. Van Duyne, *J. Phys. Chem. B*, 2005, **109**, 11279–11285.
37 J. Nelayah, M. Kociak, O. Stephan, F. J. García de Abajo, M. Tence, L. Henrard, D. Taverna, I. Pastoriza-Santos, L. M. Liz-Marzán and C. Colliex, *Nat. Phys*., 2007, **3**, 348–353.
38 R. A. Álvarez-Puebla, D. J. Ross, G. A. Nazri and R. F. Aroca, *Langmuir*, 2005, **21**, 10504–10508.

